

Notes on Spectral Analysis

Lars Umlauf and Eefke van der Lee

August 19, 2010

1 Introduction

These notes provide a condensed presentation of the classical spectral techniques typically used for the analysis of geophysical (and other) data sets. They will be useful for undergraduate students looking for a short and concise presentation of this material supplementary to their classes in fluid mechanics and turbulence. The notes start from scratch and require only some basic mathematical knowledge about complex numbers and Fourier analysis. Approaches based on Fourier series for periodic functions and Fourier transforms for non-periodic functions are discussed, and their relations are highlighted.

In the context of this material we provide some MATLAB routines with numerical implementations of the techniques discussed in the following. We appreciate any feedback, in particular regarding typos and errors.

2 Fourier Transforms

Consider a complex function, $g(x) \in \mathbb{C}$, that can be represented in the form

$$\begin{aligned} g(x) &= \int_{-\infty}^{\infty} \hat{g}(\kappa) e^{i\kappa x} d\kappa, \\ \hat{g}(\kappa) &= \frac{1}{2\pi} \int_{-\infty}^{\infty} g(x) e^{-i\kappa x} dx, \end{aligned} \tag{1}$$

where $\hat{g}(\kappa) \in \mathbb{C}$ denotes the Fourier transform of $g(x)$. The functions $g(x)$ and $\hat{g}(\kappa)$ are said to form a *Fourier transform pair*. Here, $e^{i\kappa x}$ represents a *Fourier mode* with *wave number*, κ , corresponding to the *wave length*, λ , according to $\kappa = 2\pi/\lambda$.

Fourier modes obey the *orthogonality relation*,

$$\delta(\kappa - \kappa') = \frac{1}{2\pi} \int_{-\infty}^{\infty} e^{-i(\kappa - \kappa')x} dx, \tag{2}$$

where $\delta(\kappa - \kappa')$ appearing in (2) denotes the *Dirac delta distribution*, the properties of which are discussed in Section B. Using (2), the validity of (1) is easily shown, which, however, does not prove that the integral in (1) always exists since we have not proven convergence.

2.1 Real functions

If $g(x)$ is real, the second of (1) can be used to show that

$$g(x) \in \mathbb{R} \quad \Rightarrow \quad \hat{g}(-\kappa) = \hat{g}^*(\kappa) , \quad (3)$$

where \hat{g}^* denotes the complex conjugate of \hat{g} . This property is sometimes referred to as *conjugate symmetry*.

2.2 Symmetric functions

If $g(x)$ is symmetric, it is easy to show that also its Fourier transform is symmetric,

$$g(x) = g(-x) \quad \Rightarrow \quad \hat{g}(-\kappa) = \hat{g}(\kappa) . \quad (4)$$

Further, making use of Euler's relation,

$$e^{i\kappa x} = \cos(\kappa x) + i \sin(\kappa x) , \quad (5)$$

relation (1) can be re-written in the form

$$\begin{aligned} g(x) &= 2 \int_0^\infty \hat{g}(\kappa) \cos(\kappa x) \, d\kappa , \\ \hat{g}(\kappa) &= \frac{1}{\pi} \int_0^\infty g(x) \cos(\kappa x) \, dx , \end{aligned} \quad (6)$$

which follows simply from the fact that the integral of the product of a symmetric and an antisymmetric function vanishes.

Similar relations may be obtained for the case that $g(x)$ is anti-symmetric. Note that if $g(x)$ is both real and symmetric, also its Fourier transform is real and symmetric.

2.3 Examples

In the first example we consider the Fourier transform of a symmetric rectangular window with width Δ defined according to

$$g(x) = \begin{cases} H & \text{if } |x| \leq \Delta/2 \\ 0 & \text{otherwise} \end{cases} . \quad (7)$$

Using the cosine expansion (6) for symmetric functions, it is easy to show that the Fourier transform of (7) corresponds to

$$\hat{g}(\kappa) = \frac{H \sin(\kappa\Delta/2)}{\pi \kappa} = \frac{1 \sin(\kappa\Delta/2)}{2\pi \kappa\Delta/2} , \quad (8)$$

where in the second step we have assumed that $H = 1/\Delta$, i.e. we have normalized $g(x)$ such that its integral is equal to unity. A few examples of $g(x)$ and its transform are given in Figure 1. Note that narrow windows correspond to wide Fourier transforms.

In the second example the Fourier transform of a triangular window of width Δ , i.e.

$$g(x) = \begin{cases} H \left(1 - \frac{|x|}{\Delta/2}\right) & \text{if } |x| \leq \Delta/2 \\ 0 & \text{otherwise} \end{cases} , \quad (9)$$

is investigated. This function is also known as the *Bartlett* window function.

The Fourier transform of (9) corresponds to

$$\hat{g}(\kappa) = \frac{H \sin^2(\kappa\Delta/4)}{\pi \kappa^2 \Delta/4} = \frac{1 \sin^2(\kappa\Delta/4)}{2\pi (\kappa\Delta/4)^2} , \quad (10)$$

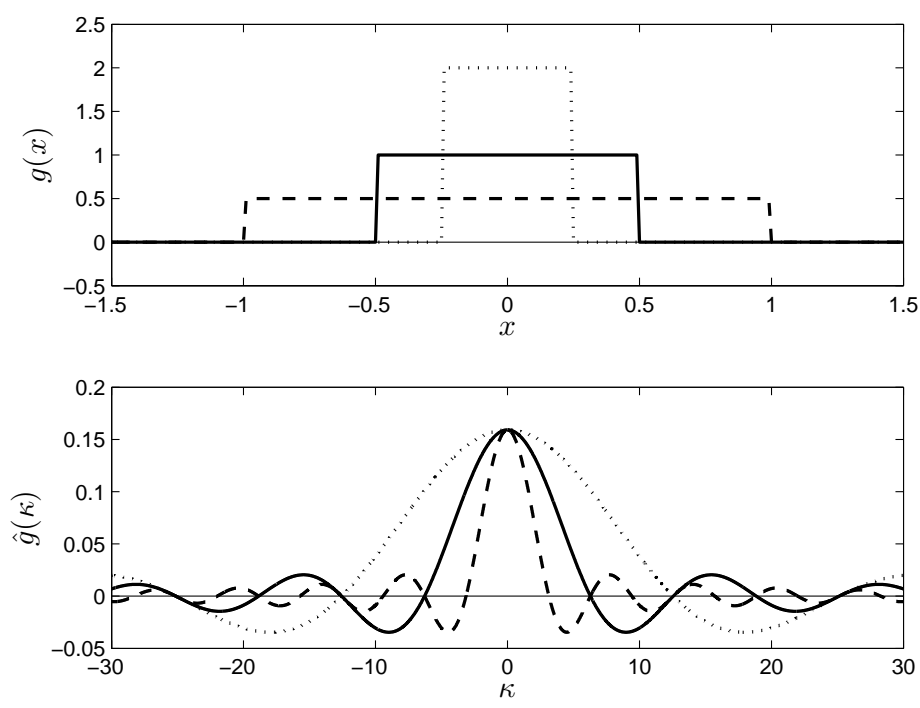


Figure 1: Function $g(x)$ and Fourier transform $\hat{g}(\kappa)$ of a symmetric box window with different $H = 1/\Delta$.

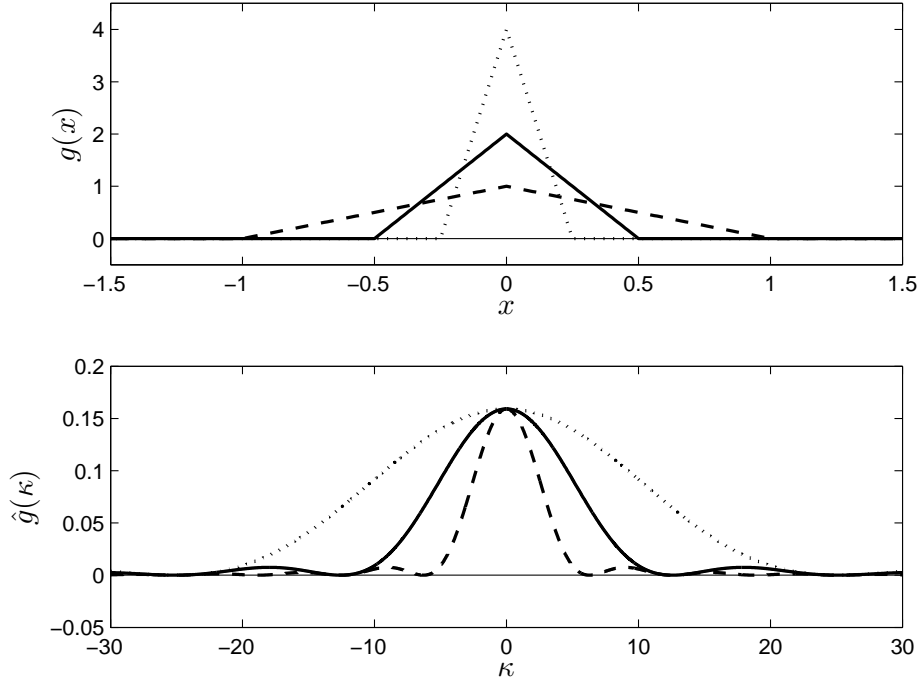


Figure 2: Function $g(x)$ and Fourier transform $\hat{g}(\kappa)$ of a symmetric Bartlett window with different $H = 2/\Delta$.

where again in the second step we have assumed that $H = 2/\Delta$ to insure that the integral of $g(x)$ is unity. A few examples of $g(x)$ and its transform are given in Figure 2. It is interesting to note that according to (1) the integral of $g(x)$ corresponds to $2\pi\hat{g}(0)$. Since the integral of $g(x)$ has been normalized to unity for the windows discussed here, we expect $\hat{g}(0) = 1/(2\pi) \approx 0.16$, corresponding to the values shown in Figure 1 and Figure 2.

3 Fourier Series

For the case that $g(x) \in \mathbb{C}$ is periodic with period L , an expansion of $g(x)$ can be found in terms of the *Fourier series*,

$$\begin{aligned} g(x) &= \sum_{n=-\infty}^{\infty} \hat{g}_n e^{i\kappa_n x} , \\ \hat{g}_n &= \frac{1}{L} \int_{-L/2}^{L/2} g(x) e^{-i\kappa_n x} dx . \end{aligned} \tag{11}$$

Here, \hat{g}_n denotes the *Fourier coefficient* of the n th Fourier mode, $e^{i\kappa_n x}$, with discrete wave number

$$\kappa_n = \frac{2\pi}{\lambda_n} = \frac{2\pi n}{L} , \tag{12}$$

where λ_n is the wave length. From (12) it is obvious that $\kappa_{-n} = -\kappa_n$.

Similar to the continuous case, (2), also the discrete Fourier modes can be shown to be orthogonal, i.e.

$$\frac{1}{L} \int_{-L/2}^{L/2} e^{i(\kappa_n - \kappa_m)x} dx = \langle e^{i(\kappa_n - \kappa_m)x} \rangle_L = \delta_{nm} , \tag{13}$$

where $\langle \cdot \cdot \cdot \rangle_L$ denotes the average over one period, and δ_{nm} is the *Kronecker delta* with the properties $\delta_{nm} = 1$ for $n = m$, and $\delta_{nm} = 0$ otherwise.

3.1 Real functions

For real $g(x)$, the Fourier coefficients exhibit conjugate symmetry,

$$g(x) \in \mathbb{R} \quad \Rightarrow \quad \hat{g}_{-n} = \hat{g}_n^* , \tag{14}$$

which is completely analogous to the continuous case in (3).

3.2 Symmetric functions

If $g(x)$ is symmetric it is easy to show that also the Fourier coefficients are symmetric,

$$g(x) = g(-x) \quad \Rightarrow \quad \hat{g}_n = \hat{g}_{-n} , \quad (15)$$

and $g(x)$ can be expressed in terms of the cosine expansion

$$\begin{aligned} g(x) &= \hat{g}_0 + 2 \sum_{n=1}^{\infty} \hat{g}_n \cos(\kappa_n x) , \\ \hat{g}_n &= \frac{2}{L} \int_0^{L/2} g(x) \cos(\kappa_n x) \, dx . \end{aligned} \quad (16)$$

For skew-symmetric $g(x)$, the corresponding sine expansion is easily derived.

4 Spectral decomposition of periodic functions

4.1 Real deterministic variables

Consider two periodic functions, $u(x), w(x) \in \mathbb{R}$, with period L and zero mean. The average of the product of u and w as a function of spatial separation, r , is called the *cross-covariance*, defined as

$$R_{uw}(r) = \langle u(x)w(x+r) \rangle_L , \quad (17)$$

which is a real periodic function with properties

$$R_{uw}(-r) = R_{wu}(r) . \quad (18)$$

Inserting the Fourier expansion, (11), into (17) we obtain

$$\begin{aligned}
R_{uw}(r) &= \left\langle \left(\sum_{n=-\infty}^{\infty} \hat{u}(\kappa_n) e^{i\kappa_n x} \right) \left(\sum_{m=-\infty}^{\infty} \hat{w}(\kappa_m) e^{i\kappa_m(x+r)} \right) \right\rangle_L \\
&= \sum_{n=-\infty}^{\infty} \sum_{m=-\infty}^{\infty} \hat{u}(\kappa_n) \hat{w}(\kappa_m) \langle e^{i(\kappa_n + \kappa_m)x} \rangle_L e^{i\kappa_m r} \\
&= \sum_{m=-\infty}^{\infty} \hat{u}(-\kappa_m) \hat{w}(\kappa_m) e^{i\kappa_m r} = \sum_{m=-\infty}^{\infty} \hat{u}^*(\kappa_m) \hat{w}(\kappa_m) e^{i\kappa_m r}
\end{aligned} \tag{19}$$

where we have used the orthogonality relation, (13), and, in the last step, the fact that $u(x)$ and $w(x)$ are real, and thus (14) is valid.

The cross-covariance defined in (17) may thus be written in the form

$$R_{uw}(r) = \sum_{m=-\infty}^{\infty} \hat{E}_{uw}(\kappa_m) e^{i\kappa_m r}, \quad \hat{E}_{uw}(\kappa_m) = \hat{u}^*(\kappa_m) \hat{w}(\kappa_m), \tag{20}$$

where the last relation implies that

$$\hat{E}_{uw}(-\kappa_m) = \hat{E}_{wu}(\kappa_m) = \hat{E}_{uw}^*(\kappa_m) \quad . \tag{21}$$

Note that in general \hat{E}_{uw} is complex: $\hat{E}_{uw} \in \mathbb{C}$.

4.1.1 Interpretation of the co-spectrum

The significance of \hat{E}_{uw} for real variables can be understood by re-writing its definition in (20) as

$$\hat{E}_{uw}(\kappa_m) = |\hat{u}(\kappa_m)| |\hat{w}(\kappa_m)| e^{i\Delta\varphi(\kappa_m)}, \tag{22}$$

where we defined $\hat{u} = |\hat{u}| e^{i\varphi_u}$ and $\hat{w} = |\hat{w}| e^{i\varphi_w}$ with φ_u and φ_w denoting the phase of \hat{u} and \hat{w} , respectively, and $\Delta\varphi = \varphi_w - \varphi_u$ the phase difference. Using

the symmetry relation for negative κ_m , (21), the cross-covariance defined in (20) can be expressed as

$$\begin{aligned}
R_{uw}(0) = \langle uw \rangle_L &= \sum_{m=1}^{\infty} \left(\hat{E}_{uw}(\kappa_m) + \hat{E}_{uw}^*(\kappa_m) \right) \\
&= \sum_{m=1}^{\infty} \mathcal{R}e \left(2 \hat{E}_{uw}(\kappa_m) \right) \\
&= \sum_{m=1}^{\infty} 2 |\hat{u}(\kappa_m)| |\hat{w}(\kappa_m)| \cos(\Delta\varphi(\kappa_m)) ,
\end{aligned} \tag{23}$$

where in the last step we used (22). The real part of $2\hat{E}_{uw}(\kappa_m)$ therefore represent the contribution of modes of wavenumber κ_m to the total cross-covariance between u and w . This quantity is seen to be proportional to the amplitude of the Fourier coefficients, and depends on the phase with zero covariance for a phase shift of $\Delta\varphi = \pm\pi/2$.

4.1.2 Interpretation of the spectrum

As a special case of (17) we now assume that $u = w$, which leads to the definition of the *auto-covariance*,

$$R(r) = \langle u(x)u(x+r) \rangle_L , \tag{24}$$

which is seen to be real and symmetric,

$$R(-r) = R(r) \quad . \tag{25}$$

Therefore, using (16), the Fourier expansion of $R(r)$ can be written as

$$R(r) = \sum_{m=1}^{\infty} \hat{E}(\kappa_m) \cos(\kappa_m r) , \quad \hat{E}(\kappa_m) = 2\hat{u}^*(\kappa_m)\hat{u}(\kappa_m) , \tag{26}$$

and, since $R(r)$ is real and symmetric, also its Fourier coefficients are real and symmetric,

$$\hat{E}(-\kappa_m) = \hat{E}(\kappa_m) = \hat{E}^*(\kappa_m) \quad . \tag{27}$$

Evaluating (26) for the case $r = 0$,

$$R(0) = \langle u^2 \rangle_L = \sum_{m=1}^{\infty} \hat{E}(\kappa_m), \quad (28)$$

it is clear that $\hat{E}(\kappa_m)$ represents the contribution of the m th Fourier mode to the variance, $\langle u^2 \rangle_L$. If u is interpreted as a velocity, $\hat{E}(\kappa_m)$, would therefore be proportional to the *energy* contained in mode m .

4.2 Real, stochastic variables

As in the previous section, we assume also here that $u(x), w(x) \in \mathbb{R}$, are two periodic functions with period L . Now, however, we consider $u(x)$ and $w(x)$ as realizations of two *stochastic processes*. The *ensemble average* over an infinite number of such realizations is denoted by the symbol $\langle \cdot \cdot \cdot \rangle$, which should not be confused with the average over one period, $\langle \cdot \cdot \cdot \rangle_L$. In the following we assume that u and w have zero mean, i.e. that $\langle u \rangle = \langle w \rangle = 0$. In addition, the process is assumed to be *homogenous*, which means that the ensemble average of any statistical quantity does not depend on x . Note that the temporal equivalent of a homogenous process is usually called a *stationary* process.

Completely analogous to (17), the cross-covariance for u and w is defined as

$$R_{uw}(r) = \langle u(x)w(x+r) \rangle, \quad (29)$$

which is a real and periodic function with properties identical to (18). We use the same symbol, R_{uw} , here for the cross-covariance for both deterministic and stochastic variables because the meaning will always be clear from the context.

Clearly, any realization, $u(x)$, of a periodic stochastic process can be represented by a Fourier series of the form (11) like any other function, with

the important difference, however, that the Fourier coefficients, $\hat{u}(\kappa_m)$, of *different* realizations of u are now stochastic variables.

Inserting Fourier expansions of the form (11) into (29) we obtain

$$\begin{aligned} R_{uw}(r) &= \left\langle \left(\sum_{n=-\infty}^{\infty} \hat{u}(\kappa_n) e^{i\kappa_n x} \right) \left(\sum_{m=-\infty}^{\infty} \hat{w}(\kappa_m) e^{i\kappa_m(x+r)} \right) \right\rangle \\ &= \sum_{n=-\infty}^{\infty} \sum_{m=-\infty}^{\infty} \langle \hat{u}(\kappa_n) \hat{w}(\kappa_m) \rangle e^{i(\kappa_n + \kappa_m)x} e^{i\kappa_m r} . \end{aligned} \quad (30)$$

Next, we use the fact that the process is homogenous by taking the average of (30) over one period. Since, obviously, $\langle R_{uw}(r) \rangle_L = R_{uw}(r)$ this yields

$$\begin{aligned} R_{uw}(r) &= \left\langle \sum_{n=-\infty}^{\infty} \sum_{m=-\infty}^{\infty} \langle \hat{u}(\kappa_n) \hat{w}(\kappa_m) \rangle e^{i(\kappa_n + \kappa_m)x} e^{i\kappa_m r} \right\rangle_L \\ &= \sum_{n=-\infty}^{\infty} \sum_{m=-\infty}^{\infty} \langle \hat{u}(\kappa_n) \hat{w}(\kappa_m) \rangle \langle e^{i(\kappa_n + \kappa_m)x} \rangle_L e^{i\kappa_m r} \\ &= \sum_{m=-\infty}^{\infty} \langle \hat{u}(-\kappa_m) \hat{w}(\kappa_m) \rangle e^{i\kappa_m r} = \sum_{m=-\infty}^{\infty} \langle \hat{u}^*(\kappa_m) \hat{w}(\kappa_m) \rangle e^{i\kappa_m r} , \end{aligned} \quad (31)$$

where we have used (13) and (14) in the second last and last step, respectively. Similar to (20), also the cross-covariance can be written as

$$R_{uw}(r) = \sum_{m=-\infty}^{\infty} \hat{E}_{uw}(\kappa_m) e^{i\kappa_m r} , \quad \hat{E}_{uw}(\kappa_m) = \langle \hat{u}^*(\kappa_m) \hat{w}(\kappa_m) \rangle , \quad (32)$$

where \hat{E}_{uw} has the properties listed in (21). The steps leading to (23) then yield

$$\begin{aligned} R_{uw}(0) = \langle uw \rangle &= \sum_{m=1}^{\infty} \mathcal{R}e \left(2 \hat{E}_{uw}(\kappa_m) \right) \\ &= \sum_{m=1}^{\infty} 2 |\langle \hat{u}(\kappa_m) \hat{w}(\kappa_m) \rangle| \cos(\Delta\varphi(\kappa_m)) , \end{aligned} \quad (33)$$

where the mean phase shift is given by $\tan(\Delta\varphi) = \mathcal{I}m(\hat{E}_{uw})/\mathcal{R}e(\hat{E}_{uw})$. The real part of (twice) the spectrum thus represents the contribution of the m th mode to the total cross-covariance.

As in (29), the auto-covariance for the stochastic process generating $u(x)$ is defined as

$$R(r) = \langle u(x)u(x+r) \rangle \quad (34)$$

which is real and symmetric as indicated in (18). The Fourier expansion of $R(r)$ is

$$R(r) = \sum_{m=1}^{\infty} \hat{E}(\kappa_m) \cos(\kappa_m r), \quad \hat{E}(\kappa_m) = 2\langle \hat{u}^*(\kappa_m)\hat{u}(\kappa_m) \rangle, \quad (35)$$

where $\hat{E}(\kappa_m)$ has the properties (27), and the same interpretation, (28), as the contribution of the m th mode to the variance of $u(x)$.

$$= \frac{|\hat{E}_{uw}(\kappa_m)|}{\hat{E}_u^{1/2}(\kappa_m) \hat{E}_w^{1/2}(\kappa_m)} \quad (36)$$

Concluding, we see that the deterministic and the stochastic cases are completely analogous with the only difference that the Fourier components in the stochastic case are stochastic variables themselves, and ensemble averaging is required for the computation of the cross- and auto-covariances defining \hat{E}_{uw} and \hat{E} , respectively.

4.3 Complex variables

As generalization of the previous sections, we assume now that the variables $u(x), w(x) \in \mathbb{C}$ are *complex*, statistically homogeneous, and have zero mean. The cross-covariance is then usually defined as

$$R_{uw}(r) = \langle u^*(x)w(x+r) \rangle, \quad (37)$$

and the auto-covariance as

$$R(r) = \langle u^*(x)u(x+r) \rangle \quad . \quad (38)$$

For both functions it easy to show that the symmetry properties compiled in (18) and (25) are replaced by their complex equivalents,

$$R_{uw}(-r) = R_{wu}^*(r) \, , \quad (39)$$

and

$$R(-r) = R^*(r) \quad . \quad (40)$$

With marginal changes, a computation similar to (30) and (31) yields

$$\hat{E}_{uw}(\kappa_m) = \langle \hat{u}^*(\kappa_m)\hat{w}(\kappa_m) \rangle \, , \quad (41)$$

and

$$\hat{E}(\kappa_m) = \langle \hat{u}^*(\kappa_m)\hat{u}(\kappa_m) \rangle = \langle |\hat{u}(\kappa_m)|^2 \rangle \, , \quad (42)$$

for the cross- and auto-spectra, respectively, which are seen to be identical to the final expression given in (32) and (35). The symmetry properties for the cross-spectrum become

$$\hat{E}_{uw}(\kappa_m) = \hat{E}_{wu}^*(\kappa_m) \, , \quad (43)$$

whereas $\hat{E}(\kappa_m)$ remains real and symmetric as in (27). Note that in contrast to the real case there is no relation between the spectral coefficients for positive and negative wave numbers.

4.3.1 Application for rotary analysis of velocity data

As an example for the application of the above results consider the complex variable

$$w(z) = u(z) + iv(z) \, , \quad (44)$$

composed of the real variables, $u(z), v(z) \in \mathbb{R}$. In a geophysical context it is helpful to think of $w(z)$ as a complex representation of a horizontal velocity vector with $u(z)$ and $v(z)$ denoting the x - and y - components varying with vertical position, z . The dependency of z may be replaced by a dependency on time, and then w can be thought of as representing a fluctuating horizontal velocity vector at a give spatial position. This does not change the following analysis.

Now we identify $w(z)$ with the n th Fourier mode, which according to (11), can be written as

$$w(z) = \hat{w}_n e^{i\kappa_n z} + \hat{w}_{-n} e^{-i\kappa_n z}, \quad (45)$$

which has a simple interpretation as the sum of two counter-rotating vectors in the complex plane. The amplitude and phase of these two vectors is given by the complex Fourier coefficients that we rewrite for the following analysis in the form

$$\hat{w}_n = A^+ e^{i\phi^+}, \quad \hat{w}_{-n} = A^- e^{i\phi^-}, \quad (46)$$

where $A^+ = |\hat{w}_n|$ and $A^- = |\hat{w}_{-n}|$ denote the amplitudes, and ϕ^+ and ϕ^- the corresponding phases. The symbols $+$ and $-$ refer to counter-clockwise and clockwise rotating components, respectively. With this definition, (45) can be rewritten as

$$w(z) = A^+ e^{i(\kappa z + \phi^+)} + A^- e^{-i(\kappa z - \phi^-)}, \quad (47)$$

which, after some manipulation, yields

$$w(z) = e^{i\alpha} \bar{w}(z), \quad \bar{w}(z) = A^+ e^{i(\kappa z + \beta)} + A^- e^{-i(\kappa z + \beta)} \quad (48)$$

with

$$\alpha = \frac{\phi^+ + \phi^-}{2}, \quad \beta = \frac{\phi^+ - \phi^-}{2}. \quad (49)$$

The geometry of the curve described by the newly defined variable $\bar{w}(z)$ in the complex plane is easily understood by computing its real and imaginary

parts, $\bar{u}(z)$ and $\bar{v}(z)$, which, from (48), leads to

$$\begin{aligned}\bar{u}(z) &= (A^+ + A^-) \cos(\kappa z + \beta), \\ \bar{v}(z) &= (A^+ - A^-) \sin(\kappa z + \beta) .\end{aligned}\tag{50}$$

Squaring and adding \bar{u} and \bar{v} yields

$$\frac{\bar{u}^2(z)}{(A^+ + A^-)^2} + \frac{\bar{v}^2(z)}{(A^+ - A^-)^2} = 1 ,\tag{51}$$

which is easily recognized as the equation for an ellipse with major and minor axis of length $A^+ + A^-$ and $A^+ - A^-$, respectively. The relation between $w(z)$ and $\bar{w}(z)$, (48), illustrates that also $w(z)$ describes an ellipse in the complex plane, however, with the major axis rotated counter-clockwise by the angle α with respect to the real (or x) axis.

From (42) and (49) it is clear that for any $n > 0$ we find $A^+ = (E(\kappa_n))^{1/2}$ and $A^- = (E(\kappa_{-n}))^{1/2}$, such that the positive and negative part of the spectrum determine the counter-clockwise and clockwise components, or, via (51), the ellipticity of the curve described by the velocity vector. Two special cases are interesting. If $A^+ \gg A^-$ (i.e. if the negative part of the spectrum is negligible for a given wave number) the velocity vector represented by w exhibits a purely circular counter-clockwise rotation. The clockwise case is analogous. If $A^+ = A^-$ (i.e. if the spectrum is symmetric) the velocity vector is rectilinear.

5 Non-periodic variables

It is evident that also for non-periodic, homogenous variables the cross- and auto-correlations can be defined exactly as in (37) and (38), respectively, with the important difference, however, that neither function is periodic any more. The spectral representation of the cross-covariance is then described by

the Fourier transform pair,

$$\begin{aligned}
R_{uw}(r) &= \int_{-\infty}^{\infty} E_{uw}(\kappa) e^{i\kappa r} d\kappa , \\
E_{uw}(\kappa) &= \frac{1}{2\pi} \int_{-\infty}^{\infty} R_{uw}(r) e^{-i\kappa r} dr .
\end{aligned} \tag{52}$$

The relations for the auto-covariance,

$$\begin{aligned}
R(r) &= \int_0^{\infty} E(\kappa) \cos(\kappa r) d\kappa , \\
E(\kappa) &= \frac{2}{\pi} \int_0^{\infty} R(r) \cos(\kappa r) dr ,
\end{aligned} \tag{53}$$

reduce to cosine expansion due to the symmetry of $R(r)$, and are seen to be similar to the corresponding expressions for the periodic case. Also similar is the interpretation for the special case with $r = 0$ yielding

$$R(0) = \langle u^2 \rangle = \int_0^{\infty} E(\kappa) d\kappa . \tag{54}$$

The physical interpretation of this clearly is that $E(\kappa)d\kappa$ corresponds to the variance of u contained in modes inside a wavenumber band of width $d\kappa$ centered around the wavenumber κ .

Interesting is also the analogous case obtained by setting $\kappa = 0$ in the second relation of (63), from which we obtain

$$E(0) = \frac{2}{\pi} \int_0^{\infty} R(r) dr = \langle u^2 \rangle \frac{2}{\pi} \int_0^{\infty} \rho(r) dr , \tag{55}$$

where we have introduced the dimensionless *auto-correlation function*,

$$\rho(r) = \frac{R(r)}{\langle u^2 \rangle} . \tag{56}$$

The integral of this function yields a length scale,

$$\mathcal{L} = \int_0^{\infty} \rho(r) dr , \tag{57}$$

which is a measure for the distance over which the process is auto-correlated. Therefore, \mathcal{L} is sometimes called the *correlation length*. Its relation to the value of the spectrum at zero frequency becomes clear from (65), which can be rewritten as

$$\mathcal{L} = \frac{\pi E(0)}{2 \langle u^2 \rangle} . \quad (58)$$

5.0.2 Relation between continuous and discrete spectra

Since the general, non-periodic case discussed in this section includes the periodic case, there must be a relation between the discrete form of the cospectra and spectra defined in (41) and (42), and the continuous form defined in (62) and (63). This relation is given by the expressions

$$\begin{aligned} E_{uw}(\kappa) &= \sum_{m=-\infty}^{\infty} \hat{E}_{uw}(\kappa_m) \delta(\kappa - \kappa_m) , \\ E(\kappa) &= \sum_{m=0}^{\infty} \hat{E}(\kappa_m) \delta(\kappa - \kappa_m) , \end{aligned} \quad (59)$$

which is easily checked by inserting, e.g., the first expression into (62) and exploiting the exchange property, (85), of the δ distribution. This yields

$$\begin{aligned} R_{uw}(r) &= \int_{-\infty}^{\infty} \left(\sum_{m=-\infty}^{\infty} \hat{E}_{uw}(\kappa_m) \delta(\kappa - \kappa_m) \right) e^{i\kappa r} d\kappa , \\ &= \sum_{m=-\infty}^{\infty} \hat{E}_{uw}(\kappa_m) \int_{-\infty}^{\infty} \delta(\kappa - \kappa_m) e^{i\kappa r} d\kappa , \\ &= \sum_{m=-\infty}^{\infty} \hat{E}_{uw}(\kappa_m) e^{i\kappa_m r} , \end{aligned} \quad (60)$$

which is seen to coincide with (32). The computation for the autospectrum, $E(\kappa)$, is analogous.

A more direct relation between the discrete and continuous forms of the spectra is obtained by integrating (59) around a small wavenumber range in the vicinity of κ_m ,

$$\hat{E}_{uw}(\kappa_m) = \int_{\kappa_m - \Delta\kappa/2}^{\kappa_m + \Delta\kappa/2} E_{uw}(\kappa) d\kappa \approx E_{uw}(\kappa_m)\Delta\kappa \quad (61)$$

where $\Delta\kappa = 2\pi/L$ is the formal frequency resolution for variables with period L obtained from (12).

6 Non-periodic variables

It is evident that also for non-periodic, homogenous variables the cross- and auto-correlations can be defined exactly as in (37) and (38), respectively, with the important difference, however, that neither function is periodic any more. The spectral representation of the cross-covariance is then described by the Fourier transform pair,

$$\begin{aligned} R_{uw}(r) &= \int_{-\infty}^{\infty} E_{uw}(\kappa) e^{i\kappa r} d\kappa , \\ E_{uw}(\kappa) &= \frac{1}{2\pi} \int_{-\infty}^{\infty} R_{uw}(r) e^{-i\kappa r} dr . \end{aligned} \quad (62)$$

The relations for the auto-covariance,

$$\begin{aligned} R(r) &= \int_0^{\infty} E(\kappa) \cos(\kappa r) d\kappa , \\ E(\kappa) &= \frac{2}{\pi} \int_0^{\infty} R(r) \cos(\kappa r) dr , \end{aligned} \quad (63)$$

reduce to cosine expansion due to the symmetry of $R(r)$, and are seen to be similar to the corresponding expressions for the periodic case. Also similar is the interpretation for the special case with $r = 0$ yielding

$$R(0) = \langle u^2 \rangle = \int_0^{\infty} E(\kappa) d\kappa \quad . \quad (64)$$

The physical interpretation of this clearly is that $E(\kappa)d\kappa$ corresponds to the variance of u contained in modes inside a wavenumber band of width $d\kappa$ centered around the wavenumber κ .

Interesting is also the analogous case obtained by setting $\kappa = 0$ in the second relation of (63), from which we obtain

$$E(0) = \frac{2}{\pi} \int_0^\infty R(r) dr = \langle u^2 \rangle \frac{2}{\pi} \int_0^\infty \rho(r) dr , \quad (65)$$

where we have introduced the dimensionless *auto-correlation function*,

$$\rho(r) = \frac{R(r)}{\langle u^2 \rangle} . \quad (66)$$

The integral of this function yields a length scale,

$$\mathcal{L} = \int_0^\infty \rho(r) dr , \quad (67)$$

which is a measure for the distance over which the process is auto-correlated. Therefore, \mathcal{L} is sometimes called the *correlation length*. Its relation to the value of the spectrum at zero frequency becomes clear from (65), which can be rewritten as

$$\mathcal{L} = \frac{\pi E(0)}{2 \langle u^2 \rangle} . \quad (68)$$

7 Fourier filtering

A series of useful filtering routines are based on the decomposition of a signal into Fourier components. The general idea of this approach is to multiply different Fourier components (e.g. those corresponding to high wave numbers) with damping factors and reconstruct the signal via the inverse Fourier transform. We present these methods here in terms of Fourier series (rather than Fourier transforms) since their numerical implementation described in Appendix A below relies on the assumption of periodicity. The derivation in

terms of Fourier transforms for non-periodic functions is, however, completely analogous.

In physical space, filtering of a periodic function $u(x)$ with period L can be described as a *convolution* of the form

$$\bar{u} = \int_{-L/2}^{L/2} u(x-s)g(s) ds, \quad (69)$$

where the overbar denotes filtering, and $g(s)$ is the (periodic) filter window. The expression in (69) can be imagined as a weighted average of $u(x)$ computed over the width of the moving window.

Examples of filtering windows are given in Figure 1 and Figure 2 above. Since we expect that filtering does not change a *constant* function, it is clear from (69) that

$$\int_{-L/2}^{L/2} g(s) ds = 1. \quad (70)$$

Expressing the integral in (69) in terms of the average defined in (13), we write

$$\bar{u} = L \langle u(x-s)g(s) \rangle_L, \quad (71)$$

and point out that (71) is similar in form to the cross-correlation defined in (17). After a short computation, completely analogous to that in (19), we therefore find

$$\bar{u} = L \sum_{m=-\infty}^{\infty} \hat{g}(\kappa_m) \hat{u}(\kappa_m) e^{i\kappa_m x}. \quad (72)$$

Filtering windows are generally assumed to be real and symmetric, and thus their Fourier coefficients are real, $\hat{g}^* = \hat{g}$, and symmetric. The most important conclusion from (72) is that filtering amounts to multiplying the Fourier coefficients of u with the Fourier coefficients of the filter window, \hat{g} . The advantage of working in Fourier space is based on the fact that the numerical implementation of the convolution in (71) is expensive, whereas rather

efficient algorithms exist of the discrete Fourier transform required for the implementation of (72).

As an example, we consider the Fourier coefficients of the Bartlett window described in (9) (see Figure 2). Assuming periodicity of this symmetric function, it is straightforward to show from (16) that the Fourier coefficients are of the form

$$\hat{g}(\kappa_m) = \frac{1}{L} \frac{\sin^2(\kappa_m \Delta/4)}{(\kappa_m \Delta/4)^2} . \quad (73)$$

Comparison with (10) reveals that the difference between Fourier transform and Fourier series amounts to replacing the factor $1/(2\pi)$ by $1/L$. According to (72), the amplitude of a Fourier mode with wave number κ_m is reduced by the factor $L\hat{g}(\kappa_m)$, which is often referred to as the *transfer function*.

For the example given in Figure 3, the signal contains only one single wavenumber $\kappa = 2\pi$. According to (73), the transfer function for a filter of width $\Delta = 1$ (corresponding to the wave length of the signal) is $L\hat{g} = 0.405$. A damping by this factor is confirmed by the filtered signal displayed in the upper panel of Figure 3.

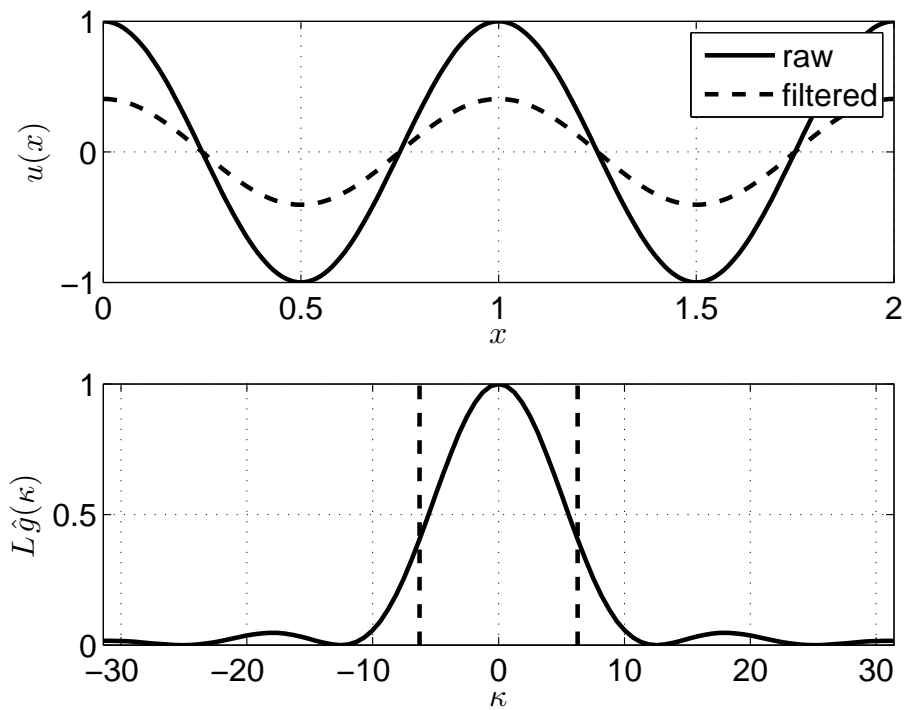


Figure 3: Raw and filtered signals (upper panel), and Fourier transform $\hat{g}(\kappa_m)$ of the Bartlett filtering window (lower panel). The vertical dashed lines in the lower panel indicate the wave number κ_m of the signal.

A Discrete Fourier Transform

Physical data are always sampled at discrete positions, $x_k = k\Delta x$, where Δx is the sampling interval, assumed to be constant here for simplicity, and k is an integer in the range $k = 0 \dots N - 1$. Sampling a continuous variable, w , at the positions x_k yields discrete samples, $w_k = w(x_k)$, defined inside the interval $0 \leq x_k < L$, where, as before, $L = N\Delta x$, denotes the period.

For even N the discrete form of the Fourier series, (11), is then defined according to

$$\begin{aligned} w_k &= \sum_{n=1-N/2}^{N/2} \hat{w}_n e^{i\kappa_n t_k} = \sum_{n=1-N/2}^{N/2} \hat{w}_n e^{2\pi i n k / N}, \\ \hat{w}_n &= \frac{1}{N} \sum_{k=0}^{N-1} w_k e^{-i\kappa_n t_k} = \frac{1}{N} \sum_{k=0}^{N-1} w_k e^{-2\pi i n k / N}, \end{aligned} \quad (74)$$

where the definition of the wave number given in (12) has been used. A very similar relation can be derived for odd values of N . The consistency of (74) is can be confirmed by making use of the relation

$$I_{j,N} = \frac{1}{N} \sum_{n=1-N/2}^{N/2} e^{2\pi i j n / N} = \begin{cases} 1 & \text{if } j/N \text{ is an integer} \\ 0 & \text{otherwise.} \end{cases} \quad (75)$$

which is recognized as the discrete version of the orthogonality relation, (13). The proof of this is left as an exercise to the reader.

A.1 Alternative form of the DFT

Some programming languages like MATLAB do not allow negative indexing. Therefore, often an alternative form of the discrete Fourier transform pair is

used,

$$\begin{aligned}
w_k &= \frac{1}{N} \sum_{n=0}^{N-1} \hat{w}_n^* e^{2\pi i n k / N} , \\
\hat{w}_n^* &= \sum_{k=0}^{N-1} w_k e^{-2\pi i n k / N} ,
\end{aligned} \tag{76}$$

which is equivalent to (74). This equivalency and the relation between the Fourier coefficients \hat{w}^* and \hat{w} is easily established from re-arranging the representation of w_k in (74) as

$$\begin{aligned}
\sum_{n=1-N/2}^{N/2} \hat{w}_n e^{2\pi i n k / N} &= \sum_{n=0}^{N/2} \hat{w}_n e^{2\pi i n k / N} + \sum_{n=1-N/2}^{-1} \hat{w}_n e^{2\pi i n k / N} \\
&= \sum_{n=0}^{N/2} \hat{w}_n e^{2\pi i n k / N} + \sum_{m=N/2+1}^{N-1} \hat{w}_{m-N} e^{2\pi i (m-N) k / N} \\
&= \sum_{n=0}^{N/2} \hat{w}_n e^{2\pi i n k / N} + \sum_{m=N/2+1}^{N-1} \hat{w}_{m-N} e^{2\pi i m k / N} e^{-2\pi i k} ,
\end{aligned} \tag{77}$$

where we have introduced the shifted index $n = m - N$. Using the fact that

$$e^{-2\pi i k} = 1 , \tag{78}$$

a comparison of (76) and the last row of (77) yields

$$\begin{aligned}
w_k &= \frac{1}{N} \sum_{n=0}^{N-1} \hat{w}_n^* e^{2\pi i n k / N} \\
&= \sum_{n=0}^{N/2} \hat{w}_n e^{2\pi i n k / N} + \sum_{n=N/2+1}^{N-1} \hat{w}_{n-N} e^{2\pi i n k / N} ,
\end{aligned} \tag{79}$$

illustrating that (74) and (76) are equivalent if the relation

$$\hat{w}_n^* = \begin{cases} N\hat{w}_n & \text{for } 0 \leq n \leq N/2 \\ N\hat{w}_{n-N} & \text{for } N/2 + 1 \leq n \leq N-1 \end{cases} \tag{80}$$

holds. In this context it is worth recalling from the Nyquist theorem that Fourier modes with wave lengths smaller than $2\Delta x$ cannot be resolved. Since these modes occur for all $n > N/2$, it appears, on the first glance, that the summation in the first line of (76) is invalid for indices exceeding this value. This paradoxon is easily resolved from the relation

$$e^{i\kappa_n t_k} = e^{i\kappa_{n-N} t_k} \quad \text{for} \quad N/2 + 1 \leq n \leq N - 1, \quad (81)$$

which follows directly from (78), and illustrates that wave numbers for modes with $n > N/2$ correspond in fact to the modes with negative wave numbers in (74). Mathematically, the modes are sampled with double frequency (illustrated by the factor $e^{2\pi i n} = 1$, and appear as low frequency modes. This effect is called aliasing, and is investigated a bit closer in the following section.

A.2 Aliasing

As mentioned above, no Fourier modes with wave lengths smaller than the so-called Nyquist wave length, $2\Delta x$, can be directly resolved by the discrete Fourier transform. According to (12) this corresponds to a Nyquist wave number of

$$\frac{\kappa_N}{2} = \frac{\pi}{\Delta x}, \quad (82)$$

where κ_N is the sampling wave number. If the signal that is sampled contains also higher wave numbers an effect occurs that *aliases* this energy to the resolved modes. How this works can be seen from the following arguments.

For any Fourier mode m with $m > N/2$, i.e. exceeding the Nyquist wave number, it is obvious that always a mode can be found such that $n = m - rN$ with n in the resolved range $-N/2 + 1 \leq n \leq N/2$, and r denoting a positive integer. For such modes it follows that

$$\hat{w}_n e^{i\kappa_n t_k} = \hat{w}_n e^{i\kappa_{m-rN} t_k} = \hat{w}_n e^{i\kappa_m t_k} e^{-ir\kappa_N t_k} = \hat{w}_n e^{i\kappa_m t_k}, \quad (83)$$

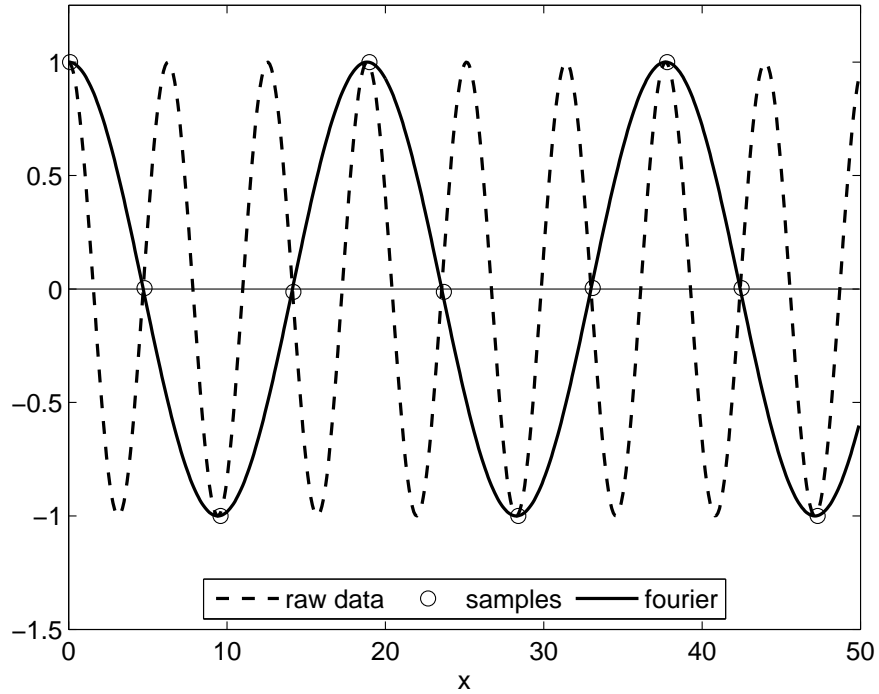


Figure 4: Example of aliasing of a raw signal (dashed line) by undersampling (circles) creating a false frequency (solid line).

where we have used (12) and (78). Thus, the energy contained in the Fourier components of the unresolved mode m will be found in the resolved mode n , which may have a much lower frequency. An example is shown Figure 4.

B The Dirac delta-distribution

Here comes the short version. Imagine the δ -distribution or *Dirac* δ function as an infinitely narrow, positive spike with unit area under the integral,

$$\int_{-\infty}^{\infty} \delta(x) dx = 1 \quad . \quad (84)$$

It has the following property

$$f(x') = \int_{-\infty}^{\infty} f(x) \delta(x - x') dx \quad , \quad (85)$$

where $f(x)$ is some arbitrary test function.